HHS Public Access

Author manuscript

Chem Commun (Camb). Author manuscript; available in PMC 2015 August 21.

Published in final edited form as:

Chem Commun (Camb). 2015 August 18; 51(70): 13458–13461. doi:10.1039/c5cc03910j.

Sealed Rotors for *In Situ* High Temperature High Pressure MAS NMR†

Jian Zhi Hu*, **Mary Y. Hu**, **Zhenchao Zhao**, **Suochang Xu**, **Aleksei Vjunov**, **Hui Shi**, **Donald M. Camaioni**, **Charles H. F. Peden**, and **Johannes A. Lercher**

Pacific Northwest National Laboratory, Richland, WA 99352, USA

Abstract

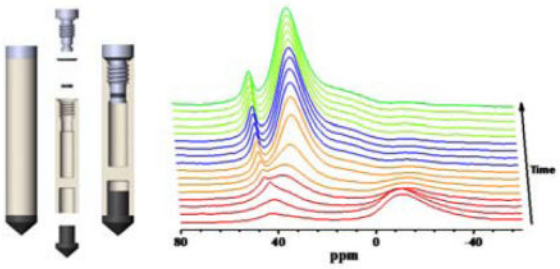

Here we present the design of reusable and perfectly-sealed all-zircornia MAS rotors. The rotors are used to study $AlPO_4$-5 molecular sieve crystallization under hydrothermal conditions, high temperature high pressure cyclohexanol dehydration reaction, and low temperature metabolomics of intact biological tissue.

MAS NMR is a powerful technique for studying structure and dynamics in solid, semi-solid, or heterogeneous systems containing mixtures of e.g., solid, semi-solid, liquid, and gaseous phases.[1–4] Due to its intrinsic advantage of probing local structure at molecular level, MAS NMR is an attractive tool for *in situ* investigations of reaction kinetics and intermediates associated with material synthesis or chemical reactions using solid catalysts where often reaction intermediates or transient species only exist under *in situ* conditions, and also an important analytical method in metabolomics.[5–13] However, the commercially available reusable-MAS rotors are rarely capable of achieving 100% seal while fast spinning even at ambient conditions. In particular, reusable sample cells that can efficiently perform at combined high temperature (> 100 °C) and high pressure (> 10 atm) conditions have not been realized in MAS NMR[14–16] due to technical complications associated with sealing heterogeneous solid/fluid/gaseous samples at high temperature and pressure while spinning at a several kHz or more inside a strong magnetic field. This limitation leaves a large territory of scientific problems related to catalytic reactions and material synthesis unexplored by *in situ* MAS NMR. Therefore, design of a perfectly sealed rotor is critically

†Electronic Supplementary Information (ESI) available: The experimental details, data process, *in situ* ^{13}C MAS NMR spectra for H-Bea catalysts, table of reaction kinetic data, attributions in ^{1}H MAS NMR spectrum of mouse-liver. See DOI: 10.1039/x0xx00000x

*Jianzhi.Hu@pnnl.gov.

needed for gaining chemical insights in related systems under *in situ* conditions.[17] Recently we were able to develop reusable MAS NMR rotors for high pressure MAS NMR and circumvent the associated technical difficulties by gluing two pieces of plastic bushing into abraded inner surface of a commercial zirconia rotor cylinder such that sealing valves and O-rings could be mounted into the bushings to create the desired high pressure seal.[18, 19] However, the weakening of the glue associated with the expansion and shrinkage of plastic bushings during variable temperature operation renders such designs unsuitable for the combined high/low temperature and high pressure conditions. To address this complication we initially used a MACOR (an easily machineable ceramic) insert for a commercial 9.5 mm Zirconia MAS rotor thus achieving an operation temperature as high as 135 °C. This system was demonstrated by performing *in situ* studies of aqueous cylcohexanol dehydration reactions.[20] However, MACOR is fragile and cannot withstand pressures above 5–10 bar. In addition, the insert also reduces the effective sample volume, which leads to a decrease in NMR sensitivity.

Herein, we report a perfectly sealed MAS rotor for a wide-range of MAS NMR experiments where samples need to be sealed.[14–21] The MAS rotors (sizes ranging from 9.5 to 3.2 mm) are fabricated using ceramics, e.g. zirconia, with the exception of the O-ring and a spin tip, such that all parts exhibit high mechanical strength. The reported rotors are easy to operate, similar to a commercial rotor, and are reusable for hundreds of times without degradation in performance. The rotor is potentially capable of operating at high pressures exceeding 100 bar and temperatures exceeding 250 °C.

As is illustrated in Figure 1, the rotor body is machined from a single block of high mechanical strength zirconia. The zirconia components are machined using diamond grinding tools. The rotor cylinder includes an opening at the top and a beveled edge or well that surrounds the opening referred to as an O-ring support. The inner bore is machined to a selected depth that defines the sample cell volume for a given rotor size. Screw threads extend from the opening at the top of the rotor body along the length of the inner wall above the sample compartment. A threaded screw zirconia cap is introduced through a high temperature O-ring into the opening at the top end of the rotor cylinder. When the screw cap is screwed into position at the top end of the rotor cylinder, the high-temperature O-ring seats onto the O-ring support above the opening and seals a sample within the cell. The screw cap may include either an extruded (Figs. 1a and 1b) or socket hexagonal-shaped (Fig. 1c) head that assists rotation into the threads of the rotor cylinder that seals the sample compartment. In an alternative design, the screw cap may seat two O-rings, a first O-ring, e.g., at a lower end near the tip of the screw cap that seats immediately above the sample compartment in the rotor cylinder to prevent samples entering into the threads and a second O-ring that seats on the O-ring support positioned at the top end of the rotor cylinder (Figs. 1b and 1c). The platform using either square threads or modified sharp-V threads with rounded corners to ensure high mechanical strength of the threads in both the zirconia rotor cylinder and the zirconia sealing screw cap have been realized. In such designs, the sample compartment is integrated with the rotor cylinder without using any glue (epoxy) and plastic bushings. Details on the dimension and the materials of each component for a representative 7.5 mm zirconia MAS rotor are provided in the supporting information. Test outside of the

magnetic field was carried out successfully by sealing pure liquid water with volume about 70% of the sample cell space of the MAS rotor and directly heating the sealed rotor system inside a closed oven all the way to the temperature limit of the oven, i.e., 245 °C for one hour. At the end of the test, the weight of the H_2O was 100% retained, i.e., without any leakage. At 245 °C, the vapor pressure of H_2O is 35 atm. The test clearly indicates that the all zirconia MAS rotor can successfully withstand 245 °C and 35 atm, a record that has never been realized previously in the history of MAS NMR. A separate outside magnet test by pressurizing the rotor to 100 bar with CO_2 at room temperature and then seal it, we found that the rotor can hold CO_2 without CO_2 leakage for more than 10 hours. As examples of versatile applications of the rotors, a square thread extended hex rotor (Figure 1a) with outside diameter 7.5 mm and cell volume 300 μL is used, and *in situ* NMR investigations of $AlPO_4$-5 crystallization, cyclohexanol dehydration reaction in homogeneous and heterogeneous phases, and metabolic profiling of intact biological tissues are carried out.

$AlPO_4$-5 molecular sieve synthesized in the rotor under *in situ* condition shows the same XRD patterns as that synthesized in the autoclave (Figure S1). *In situ* ^{27}Al and ^{31}P MAS NMR spectra and the relative signal intensity changes as a function of synthesis time are shown in Figure 2. At progressively elevated temperatures (25–150°C), six-coordinated aluminums near −11 ppm change into four-coordinated aluminums near 43 ppm, and then the peak shifts to 33 ppm represented by the framework aluminum of $AlPO_4$-5 at 110 min.[22, 23] Five-coordinated Al bonded to HPO_4^{2-} ions appears initially at 43 ppm and shift to 48 ppm (810 min) due to the change of the environment of the solution during the crystallization process, and simultaneously, a broad peak attributed to octahedral Al species bonded to HPO_4^{2-} ions appears at 12 ppm.[24, 25] The shift of ^{27}Al peaks results from the gradual adjustment of local structures of amorphous phase to form crystalline $AlPO_4$-5 by adjusting the Al-O-P bond length and angle.[26, 27] The broad peaks in ^{31}P spectra (Figure 2c), composed of partially connected phosphorus (P(OAl), $P(OAl)_2$, $P(OAl)_3$), shift from −12 to −20 ppm as more OAl connected phosphorus are formed due to condensation reaction between P and Al, and finally change into −30 ppm peak corresponding to framework phosphorus of $AlPO_4$-5.[22, 28] The sharp peak at −0.2 ppm shifts to −1.5 ppm belonging to dissolved phosphate exchanging with different aluminophosphate complex.[29] ^{27}Al and ^{31}P spectra both show significant changes occur during the first 120 min synthesis at 150 °C. Total signal intensities of ^{27}Al increase about 45% due to the formation of more homogeneous environment of ^{27}Al (Figure 2b) as more Al sites are detected (at early stage of synthesis, a part of the Al-sites have peaks that are too broad or too scattered in ppm to be detected). While the total ^{31}P signal decrease about 20% in the first 110 min due to the formation −30 ppm ^{31}P (Figure 2d), which has long relaxation time. Thanks to magic angle spinning, the different peaks resulting from difference species both in solid and liquid phase can be well distinguished. The quadrupole coupling constants of tetrahedral and octahedral coordinated Al are similar and small, i.e., 0.2–0.3 MHz, and thus relatively quantitative information from these species can be extracted by spectrum deconvolution (see supporting information).[30] Based on quantitative analysis results, six-coordinated aluminum at −13 ppm changes into four coordinated framework aluminum of $AlPO_4$-5 at 33 ppm (Figure 2b), and partially connected phosphates at −14 to −20 ppm become framework P of $AlPO_4$-5 at −30 ppm (Figure 2d). Very weak fluctuation change of

phosphate in liquid phase (−0.5— −1.5 ppm) at the very initial stage may result from mass transportation between solid gel and liquid solution during nucleation stage. Excess aluminum and phosphate with no obvious change are expelled from amorphous gel and form aluminophosphate species at 45 and 12 ppm in ^{27}Al spectra and phosphate near −1.5 ppm in ^{31}P spectra. These results imply that $AlPO_4$-5 molecular sieve is formed by rearrangement of local structure of amorphous precursor without participation of prefabricated sub-unit building blocks in solution.

In situ ^{13}C MAS NMR following cyclohexanol dehydration reaction catalyzed by H_3PO_4 and H-Beta were also performed. Figure 3 shows the stacked *in situ* ^{13}C MAS NMR plot containing 80 individual spectra acquired for the H_3PO_4 catalyzed dehydration reaction at 160 °C. In the initial reaction phase, the signal intensity observed at 125 and 128 ppm, respectively, corresponding to gas phase and dissolved 1-^{13}C-cyclohexene increases steadily as the reaction progresses. Simultaneously, we observe the decrease of signal intensity at 70.8 ppm, which is assigned to 1-^{13}C-cyclohexanol dissolved in water. Towards reaction completion, a small amount of 1-^{13}C-cyclohexene in condensed phase is observed at 126 ppm. While in the case of the HBEA catalyzed reaction (Figure S3), the NMR signal corresponding to 1-^{13}C-cyclohexene first increases to maximum and then decreases gradually, and the signal of 1-^{13}C-cyclohexanol decreases significantly at the end of reaction accompanied with the enhancement of the signals at 20 – 40 ppm (see supporting information for detailed assignments). It means that the ^{13}C-isotope scrambling of 1-^{13}C-cyclohexanol, 1-^{13}C-cyclohexene, and cyclohexene hydration back reaction are more significant in H-Beta catalyst, which is probably due to cyclohexyl carbenium as intermediate species exists in zeolite catalyst.[20] To demonstrate that the experimental results obtained using the *in situ* NMR method are comparable with those obtained using a traditional batch autoclave, we report the turnover frequency (TOF) of cyclohexanol dehydration to cyclohexene at different temperatures and the corresponding activation energy values (Figure 3b) for both the homogeneous and heterogeneous catalyst systems in Table S1. Note that while slight deviations in the TOF are observed for the homogeneous (H_3PO_4) catalyzed reaction, the determined values (approximately 148 kJ·mol^{-1}) for the activation energy are nearly identical. In the case of the zeolite-catalyzed reaction, both the reaction rate and the activation energy are very similar for both the NMR and batch autoclave reactor setups. We suggest that the minor discrepancy observed for the heterogeneous and homogeneous systems may result from the error of temperature calibration. The latter is performed in a separate experiment using ethylene glycol and assuming all experimental conditions, including spinning rate, the flow rates of the driving and bearing gases and the flow rate of the heating gases were all the same between the *in situ* experiments and the temperature calibration experiments. Unfortunately, precisely matching the experimental condition remains challenging. Nevertheless, because the determined activation barriers for the batch reactor and MAS rotor are nearly identical, we believe that kinetic data obtained by virtue of the *in situ* NMR are reproducible for both homogeneous and heterogeneous catalytic reaction systems.

Potential application of this kind of sealed rotor in HR-MAS NMR metabolomics for intact biological tissues is also demonstrated here in Figure 4. The spectra acquired on 280 mg

mouse-liver tissue are very similar to the previously report (See supporting information for detailed attributions).[31] Varying temperature ^{1}H MAS NMR spectra of the mouse-liver from 0 °C to 25 °C indicate the rotor can perfectly seal the tissue without leak of any biofluid from low temperature to room temperature. At the same time, the well sealed rotor at low temperature can effectively prevent degradation of the biological tissues.[32] This would significantly simplify HR-MAS NMR in metabolic profiling on intact biological tissues as till now perfectly sealing an intact biological tissue for MAS NMR metabolomics is pretty challenging.

In summary, a universal design for engineering perfectly sealed MAS NMR rotor is reported that is capable of sealing a heterogeneous sample containing solid, semi-solid, gases and liquids or a mixture of them under extreme experimental conditions of combined high pressure and high temperature, or cold temperature. The versatile application in material synthesis and catalytic reactions are validated by well reproduction of the results from the traditional batch experiments. High resolution ^{1}H NMR metabolomics spectrum on intact biological tissues is obtained under low temperature at 0 °C that significantly reduce the possibility of sample degradation under fast MAS. We can expect that the newly designed sealed rotors will expand applications in many fields when both sealing the sample and MAS are needed.

Supplementary Material

Refer to Web version on PubMed Central for supplementary material.

Acknowledgments

This work was supported by the U. S. Department of Energy (DOE), Office of Basic Energy Sciences, Division of Chemical Sciences, Geosciences & Biosciences and NIH Grant NIEHS R01ES022176. All experiments were performed at the Environmental Molecular Sciences Laboratory, a national scientific user facility sponsored by the DOE's Office of Biological and Environmental Research located at Pacific Northwest National Laboratory (PNNL). PNNL is a multiprogram national laboratory operated for DOE by Battelle Memorial Institute under Contract DE-AC06-76RLO1830.

Notes and references

1. Andrew ER, Bradbury A, Eades RG. Nature. 1958; 182:1659–1659.
2. Klinowski J. Prog Nucl Magn Reson Spectrosc. 1984; 16:237–309.
3. Brown SP, Spiess HW. Chem Rev. 2001; 101:4125–4155. [PubMed: 11740929]
4. Laws DD, Bitter HML, Jerschow A. Angew Chem Int Ed. 2002; 41:3096–3129.
5. Epping JD, Chmelka BF. Curr Opin Colloid Interface Sci. 2006; 11:81–117.
6. Chmelik C, Kaerger J. Chem Soc Rev. 2010; 39:4864–4884. [PubMed: 20972502]
7. Blasco T. Chem Soc Rev. 2010; 39:4685–4702. [PubMed: 20976339]
8. Zhang W, Xu S, Han X, Bao X. Chem Soc Rev. 2012; 41:192–210. [PubMed: 21743940]
9. Ivanova II, Kolyagin YG. Chem Soc Rev. 2010; 39:5018–5050. [PubMed: 21038049]
10. Ferey G, Haouas M, Loiseau T, Taulelle F. Chem Mater. 2014; 26:299–309.
11. Dunn WB, Bailey NJ, Johnson HE. Analyst. 2005; 130:606–625. [PubMed: 15852128]
12. Tang W, Liu Y, Peng C, Hu MY, Deng X, Lin M, Hu JZ, Loh KP. J Am Chem Soc. 2015; 137:2600–2607. [PubMed: 25646600]

13. Xiao J, Hu JZ, Chen H, Vijayakumar M, Zheng J, Pan H, Walter ED, Hu M, Deng X, Feng J, Liaw BY, Gu M, Deng ZD, Lu D, Xu S, Wang C, Liu J. Nano Lett. 2015; 15:3309–3316. [PubMed: 25785550]
14. Miyoshi T, Takegoshi K, Terao T. Macromolecules. 1997; 30:6582–6585.
15. Yonker CR, Linehan JC. Prog Nucl Magn Reson Spectrosc. 2005; 47:95–109.
16. Deuchande T, Breton O, Haedelt J, Hughes E. J Magn Reson. 2006; 183:178–182. [PubMed: 16962344]
17. Aerts A, Kirschhock CEA, Martens JA. Chem Soc Rev. 2010; 39:4626–4642. [PubMed: 20949188]
18. Hoyt DW, Turcu RVF, Sears JA, Rosso KM, Burton SD, Felmy AR, Hu JZ. J Magn Reson. 2011; 212:378–385. [PubMed: 21862372]
19. Turcu RVF, Hoyt DW, Rosso KM, Sears JA, Loring JS, Felmy AR, Hu JZ. J Magn Reson. 2013; 226:64–69. [PubMed: 23220181]
20. Vjunov A, Hu MY, Feng J, Camaioni DM, Mei D, Hu JZ, Zhao C, Lercher JA. Angew Chem Int Ed. 2014; 53:479–482.
21. Loring JS, Schaef HT, Turcu RVF, Thompson CJ, Miller QRS, Martin PF, Hu JZ, Hoyt DW, Qafoku O, Ilton ES, Felmy AR, Rosso KM. Langmuir. 2012; 28:7125–7128. [PubMed: 22533894]
22. Blackwell CS, Patton RL. J Phys Chem. 1984; 88:6135–6139.
23. Lookman R, Grobet P, Merckx R, Van Riemsdijk WH. Geoderma. 1997; 80:369–388.
24. Taulelle F, Haouas M, Gerardin C, Estournes C, Loiseau T, Ferey G. Colloid Surf A-Physicochem Eng Asp. 1999; 158:299–311.
25. Mortlock RF, Bell AT, Radke CJ. J Phys Chem. 1993; 97:775–782.
26. Oliver S, Kuperman A, Ozin GA. Angew Chem Int Ed. 1998; 37:47–62.
27. Müller D, Jahn E, Fahlke B, Ladwig G, Haubenreisser U. Zeolites. 1985; 5:53–56.
28. Longstaffe JG, Chen BH, Huang YN. Microporous Mesoporous Mater. 2007; 98:21–28.
29. Vistad OB, Akporiaye DE, Taulelle F, Lillerud KP. Chem Mater. 2003; 15:1639–1649.
30. Massiot D, Bessada C, Coutures JP, Taulelle F. J Magn Reson. 1990; 90:231–242.
31. Coen M, Lenz EM, Nicholson JK, Wilson ID, Pognan F, Lindon JC. Chem Res Toxicol. 2003; 16:295–303. [PubMed: 12641429]
32. Schenetti L, Mucci A, Parenti F, Cagnoli R, Righi V, Tosi MR, Tugnoli V. Concepts Magn Reson Part A. 2006; 28:430–443.

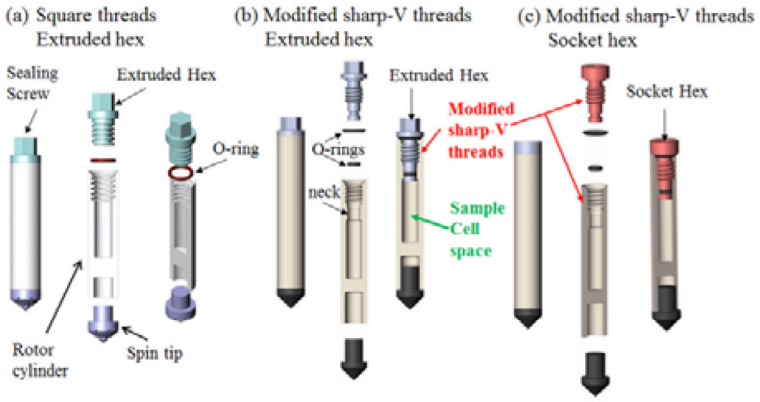

Figure 1.
Representative designs for the combined HTHP MAS NMR rotors.

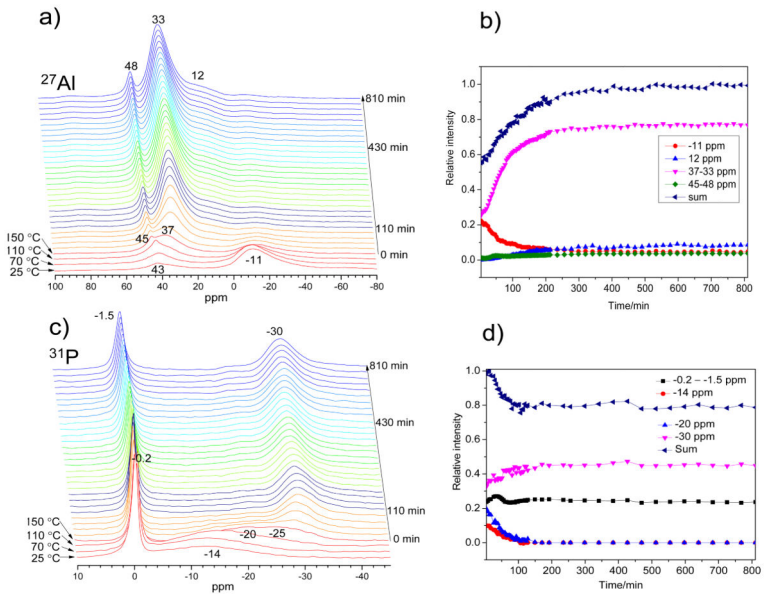

Figure 2.

In situ ^{27}Al (a) and ^{31}P (c) MAS NMR spectra of $AlPO_4$-5 molecular sieves crystallized at 150 °C as a function of the synthesis time and relative peak intensities changes as a function of synthesis time for ^{27}Al (b) and ^{31}P (d).

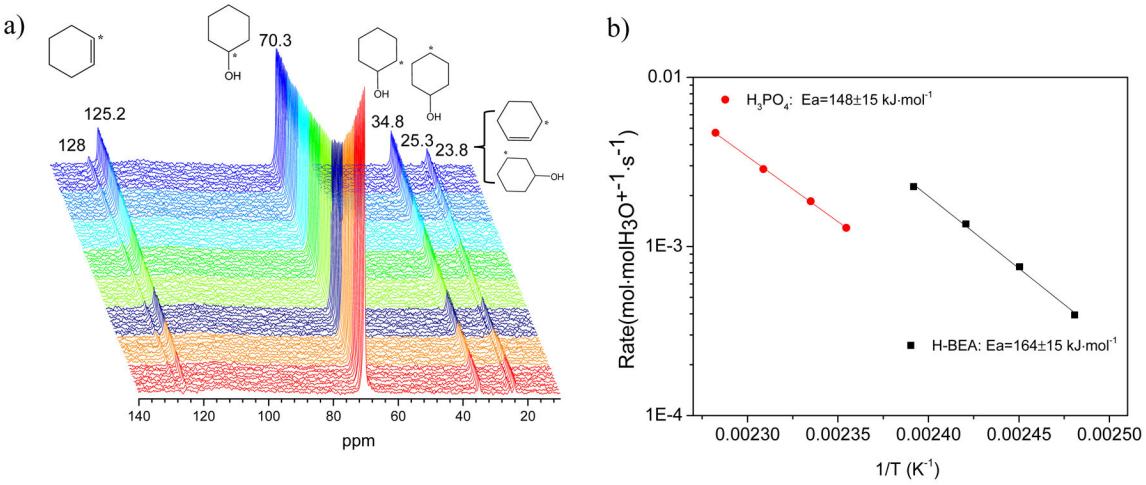

Figure 3.

Stacked plot of *in situ* ^{13}C MAS NMR spectrum of 1-^{13}C-cyclohexanol dehydration for H_3PO_4 at 160 °C (a), and Arrhenius plot of turn over frequency (TOF) of cyclohexene on H_3PO_4 and HBEA catalyst (b).

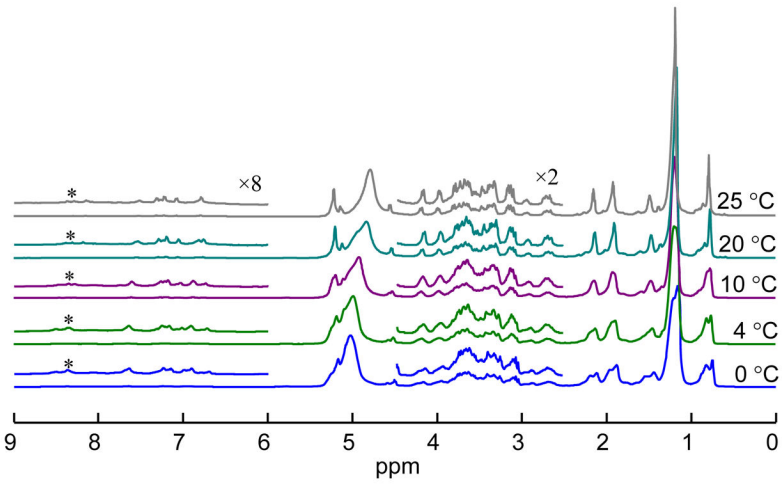

Figure 4.

Stacked plot of varying temperature ^{1}H MAS NMR spectrum of 280 mg mouse-liver from 0 °C to 25 °C.